TISSUE ENGINEERING: Part A
Volume 19, Numbers 5 and 6, 2013

DOI: 10.1089/ten.tea.2012.0480

Effective Delivery of Stem Cells Using an Extracellular Matrix Patch Results in Increased Cell Survival and Proliferation and Reduced Scarring in Skin Wound Healing

Mai T. Lam, PhD,[1] Allison Nauta, MD,[1] Nathaniel P. Meyer, BS,[1] Joseph C. Wu, MD, PhD,[2] and Michael T. Longaker, MD, MBA[1]

Wound healing is one of the most complex biological processes and occurs in all tissues and organs of the body. In humans, fibrotic tissue, or scar, hinders function and is aesthetically unappealing. Stem cell therapy offers a promising new technique for aiding in wound healing; however, current findings show that stem cells typically die and/or migrate from the wound site, greatly decreasing efficacy of the treatment. Here, we demonstrate effectiveness of a stem cell therapy for improving wound healing in the skin and reducing scarring by introducing stem cells using a natural patch material. Adipose-derived stromal cells were introduced to excisional wounds created in mice using a nonimmunogenic extracellular matrix (ECM) patch material derived from porcine small-intestine submucosa (SIS). The SIS served as an attractive delivery vehicle because of its natural ECM components, including its collagen fiber network, providing the stem cells with a familiar structure. Experimental groups consisted of wounds with stem cell-seeded patches removed at different time points after wounding to determine an optimal treatment protocol. Stem cells delivered alone to skin wounds did not survive post-transplantation as evidenced by bioluminescence *in vivo* imaging. In contrast, delivery with the patch enabled a significant increase in stem cell proliferation and survival. Wound healing rates were moderately improved by treatment with stem cells on the patch; however, areas of fibrosis, indicating scarring, were significantly reduced in wounds treated with the stem cells on the patch compared to untreated wounds.

Introduction

One of the most complex biological processes in the human body is wound healing. The process of wound repair occurs in all tissues and, interestingly, involves nearly the same sequence of events. Healing in the skin is of particular interest as the skin is the first line of defense. Additionally, reduced scarring is desired to increase tissue functionality and for improved aesthetics. The skin is composed of two layers: the epidermis and dermis. The epidermis, the outer layer, consists of a stratified epithelium and resident keratinocytes. Below the epidermis lies the dermis, containing a heterogeneous population of cells, including fibroblasts and endothelial cells, in an organized extracellular matrix (ECM). The physical characteristics of the skin are attributed to the basket-weave pattern of the collagen fibers of the dermis.[1] Disorganization of the dermis collagen fibers occurs during fibrosis, or scarring, when the fibroblasts hyperproliferate and/or produce excessive and irregular collagen.[2] Excess ECM proteins results in malfunction of the local area, affecting overall function of the tissue or organ.

The amount of resultant fibrosis depends on how a wound heals. In general, tissue defects are closed primarily using traditional sutures or staples. In cases of larger open wounds or wounds at risk of infection or contamination, primary surgical wound closure is not possible, and other options must be explored. Left unattended, wounds heal haphazardly. In cases where healing capacity is severely hindered, such as in diabetes, wounds may not heal at all. Autologous skin grafts are a treatment option, although sources of donor tissue are limited, and harvest from a donor site on the same patient can cause additional injury. Engineered skin is typically derived from differentiated cells, such as fibroblasts or keratinocytes,[3–5] which have limited proliferation capacity. It has also been suggested that these allogeneic skin substitutes merely function as a dressing with little additional benefit. In contrast, stem cells have great proliferative ability and hence

[1]Department of Surgery, Stanford University School of Medicine, Stanford, California.
[2]Departments of Radiology & Medicine, Stanford University School of Medicine, Stanford, California.

have the potential to regenerate and repair wounded tissue. Furthermore, due to stem cells' inherent multipotent properties, they have the capability to differentiate into many different tissue types, making them applicable to treatment of a wide variety of wound types. Unfortunately, it is now known that stem cells do not survive well when transplanted alone into the body, either dying or dissipating from the wound site. Attempts for aiding stem cell survival often involve coinjection with survival-promoting agents such as Matrigel or collagen gel, though the former is derived from a xenogenic tumor, and the latter does not result in significant improvement in cell survival.[6,7]

Here, we investigate use of an ECM material derived from porcine small-intestine submucosa (SIS) to promote stem cell survival and proliferation. This material provides a natural infrastructure for the stem cells to reside on. The SIS has been shown to increase vascularization of nonsplinted cutaneous wounded areas when delivered with stem cells.[8] While increased angiogenesis has been demonstrated, the effect of SIS-delivered stem cells on the rate and quality of wound repair has yet to be elucidated. Also, the effect of the SIS on enhancing stem cell application needs to be examined. The SIS-ECM serves as a familiar environment for the stem cells, potentially promoting survival and proliferation. We assessed efficacy of this approach in a mouse skin wound-healing model using adipose-derived stromal cells (ASCs). ASCs were chosen for their noncontroversial nature, abundant availability, and ease of harvest. These traits make this stem cell type potentially much faster to translate compared to other stem cell types such as embryonic stem cells. The skin wound-healing model we used closely mimics human wound healing by applying a splint around the wounded area to minimize contracture and allow the wounds to heal by granulation, as in human wounds. Treatment groups involved patch removal at varying time points after application with the ASCs to determine the ideal therapy protocol for this approach. Stem cell treatment alone did not result in improved wound healing. Wound-healing rates moderately improved with stem cell delivery with the patch. However, delivery of ASCs with the SIS patch prolonged cell survival in the wound, increased cell proliferation, and significantly decreased scarring. This simple stem cell delivery method has implications for application with other stem cell types and in other kinds of wounds.

Materials and Methods

Animals and cell isolation

All experiments were performed in accordance with the Stanford University Animal Care and Use Committee (IACUC) guidelines. The IACUC protocol number for this study was 21308. Mouse adipose-derived stromal cells (mASCs) were isolated from L2G85 male mice with a Friend leukemia virus B (FVB) strain background and ubiquitously expressed green fluorescent protein (*GFP*) and firefly luciferase (*Fluc*) reporter genes driven by a β-actin promoter as previously described.[9] Donor animals were males 8–10 weeks old. Recipient mice were syngeneic female FVB mice 10–12 weeks in age.

mASCs were isolated as previously described.[10] Briefly, the inguinal fat pads were excised from L2G85 male mice and washed twice in Betadine (Fisher Scientific, Pittsburgh, PA) and three times in phosphate-buffered saline (PBS; Invitrogen, Carlsbad, CA). Fat pads were finely minced and digested in 0.075% collagenase type II (Sigma-Aldrich, St. Louis, MO) in Hank's Balanced Salt Solution (Cellgro, Manassas, VA) for 30 min at 37°C in a shaking water bath and additionally shaken vigorously by hand every 10 min. The digest solution was neutralized with a growth medium consisting of the Dulbecco's Modified Eagle Medium (Invitrogen), 10% fetal bovine serum (Invitrogen), and 1% penicillin–streptomycin (pen-strep; Invitrogen). The cell suspension was centrifuged at 1000 rpm for 5 min, the supernatant discarded, and the cell pellet resuspended in a fresh growth media and plated. Cells of passages 1–4 were used in these experiments.

Patch material and cell seeding

The patch material was processed by Cook Biotech (West Lafayette, IN) for CorMatrix Cardiovascular, Inc. (Atlanta, GA) and is composed of porcine SIS. Briefly, porcine jejunum was cleaned by removal of the mesenteric tissues with scissors and the intestinal lumen rinsed with water for 2–5 min. The intestine was slit longitudinally and mechanically delaminated to isolate the tunica submucosa and basilar layer of the tunica mucosa, resulting in a predominantly ECM material making up the final SIS material.[11] The SIS was sterilized by ethylene oxide. The material is composed primarily of collagen type I fibers, ECM components (e.g., glycosaminoglycans and glycoproteins), and numerous growth factors (e.g., vascular endothelial growth factor, fibroblast derived growth factor-2, and transforming growth factor beta).[12] Physically, the SIS is ~155-μm thick with pore sizes up to 50 μm when hydrated.

Preliminary experiments revealed that cells do not spontaneously adhere to the SIS; hence, the material was first functionalized with the attachment protein laminin (natural mouse laminin; Invitrogen). SIS patches sized 6 mm were cut with a biopsy punch, placed in a 96-well plate, and coated with 1 μg laminin diluted in 50 μL PBS for 1 h at room temperature. Mouse ASCs at 1×10^6 cells were seeded onto each patch in 50 μL growth media. Additional medium was added 30 min after seeding to fill the well, and the cells were left to seed overnight at 37°C.

Animal wounding surgeries

A splinted excisional wounding model was used to more closely emulate human wound healing.[13] Briefly, two full-thickness skin wounds were created on the backs of each mouse. Mice were anesthetized with 2%–3% inhaled isoflurane and the fur shaved. Anesthesia was maintained with 2% inhaled isoflurane through a nose cone. Areas for wounding were disinfected with Betadine and wounds created by excising two separate 6-mm-diameter wounds per animal. These wounds were measured before excision using a 6-mm sterile excisional punch biopsy instrument (Miltex; Integra LifeSciences Corporation, York, PA). A 10-mm outer diameter and 6-mm inner diameter donut-shaped silicone splint was sutured around the wound to minimize contracture and promote re-epithelialization and deposition of granulation tissue, more closely mimicking human wound healing. The following treatments were applied to the wounds: (1) placing a patch only over the wound, (2)

applying the stem cells topically to the wound, or (3) applying patches seeded with cells. The patch only treatment was applied by first soaking plain patches in saline for ~10 min and then placing the hydrated patches over the wound. The moisture of the patch allowed it to adhere securely to the fresh wounds without further intervention. A semiocclusive dressing (Tegaderm, 3M; St. Paul, MN) was applied over the patch and wound to protect the area as it healed. The cell-seeded patch groups were similarly applied, with the only difference being the patch hydration solution (residual cell medium instead of saline). Cells alone were applied topically to the wounds and immediately covered with a dressing material to prevent drying of the cell solution. To further prevent cell loss, the wounded area was kept flat for ~15 min after cell application.

Cell-seeded patch groups included removing the patch 2 days after application (termed remove day 2); removing the patch after 6 days (termed remove day 6); and removing the patch after 2 days and replacing it with a plain noncell-seeded patch every 2 days for the remainder of experiment (termed remove and replace). The remove and replace group was created to test possible effects of the material properties alone (including the growth factors) after stem cell delivery. Patch application was continued until either the patch fell off unassisted from dehydration or could not be reapplied without intervention, such as suturing, which typically indicated that the further stages of healing had been reached. Three mice were wounded per group with two wounds per animal, equaling a total of six wounds per group. Mouse skin wounds, using the 6-mm splinted model, typically heal 14 days postwounding; thus, an additional no-treatment control group consisted of untreated wounds left to heal on their own. Wounding experiments were conducted for 14 days, since this was the point at which nontreated control wounds would heal completely unassisted. Wounds were covered with Tegaderm dressing and mice allowed to fully recover from anesthesia under a warming lamp. Animals were housed separately postsurgery.

Wound closure rates were determined by taking digital pictures of the wounds every 2 days during dressing changes. Measurements of the open wound were normalized by taking measures relative to the 6-mm silicone ring sutured around the wound. Values were reported as percent healed and calculated as follows:

$$Wound\ Area = \frac{(wound\ area/ring\ area)}{(orginal\ wound\ area/original\ ring\ area\ )}$$

Wound closure rates were reported as averages taken over six wounds per experimental group.

Material and stem cell analyses

A digital camera (Canon Powershot SD630; Canon, Lake Success, NY) was used to capture a gross image of the SIS. Scanning electron microscopy (SEM) was used to image the patch material and cellular connections to it on the micrometer level. Plain and cell-seeded SIS were sputter-coated with a 20-nm layer of Au/Pd at 10 mA, 8 V, and 70 mTorr in Argon gas. Samples were imaged with a Hitachi S-3400N variable pressure SEM (Hitachi, Tokyo, Japan). Confocal microscopy was used to determine the depth of stem cell seeding into the patch. Freshly seeded patches were slide mounted, stained with DAPI (4′,6-diamidino-2-phenylindole, dilactate; Invitrogen), and imaged using a Zeiss LSM 510 META confocal microscope (Carl Zeiss MicroImaging GmbH, Germany). A 20× objective was used in conjunction with lasers to activate the diode at a wavelength of 356 nm to excite the DAPI fluorophore (blue) and Argon to excite the green spectrum at a wavelength of 488. The cell nuclei were identified (blue light) along with the green GFP-expressing stem cells and green autofluorescent components (collagen fibrils) of the ECM.

Postwounding, stem cell survival and proliferation were tracked via bioluminescence imaging (BLI) every 2 days. In groups with patches removed on day 2 (i.e., remove day 2 and remove and replace groups), the patch was removed before imaging. Animals were anesthetized by 2%–3% inhaled isoflurane and injected intraperitoneally with the reporter probe D-Luciferin at 150 mg/kg. An IVIS Spectrum system (Xenogen, Alameda, CA) was used to image the animals while under continued 1.5%–2% inhaled isoflurane anesthesia. Each animal was scanned until the peak signal was obtained, imaging up to 30 min. Radiance was quantified in photons per second per centimeter squared per steridian. ASC luciferase activity and cell number correlation were determined by imaging cells alone in a six-well plate with D-Luciferin added to the media.

Histological analysis

On day 14 after final data collection, skin samples including and surrounding the wound area were excised. Samples were fixed in 10% neutral buffered formalin and processed for paraffin embedding. Samples were sectioned into 8-μm-thick sections and stained with hematoxylin and eosin to mark the nuclei blue, and the cytoplasm and collagen pink. Additional sections were stained using protocols for Masson's Trichrome and Picrosirius Red, to label collagen fibers blue and red, respectively. Out of about 100 sections cut per wound sample, 10 sections located near the center of the wound were selected per wound for processing. The 10 sections were evenly divided between the stains and fibrotic areas measured. Fibrosis widths and depths measured using CorelDraw software (Corel Corporation, Ottawa, Ontario, Canada) were used to calculate the fibrosis area size. Immunofluorescence was used to determine the location of any remaining transplanted ASCs in the wound after the 2-week healing period. A Zeiss Axioplan 2 fluorescence microscope was used to image the slides (Carl Zeiss, Inc., Thornwood, NY).

Cell GFP signal was amplified with an anti-GFP antibody conjugated to Alexa Fluor 488 (Invitrogen) and counterstained with DAPI. Slides were mounted with the Vectashield Mounting Medium (Vector Laboratories, Burlingame, CA) and coverslipped. For studying early time points, wound samples from the remove day-6 group were also stained with anti-GFP antibody to determine transplanted cell presence.

Statistics

Histological samples were pooled. All averages were calculated as mean values ± standard deviation. Statistical significance was determined with one-way ANOVA tests

with an alpha value of 0.05. Tukey *post hoc* analysis was performed to ascertain significance between groups, with p-values < 0.05.

Results

Material structure and stem cell characterization

A gross image shows the overall structure of the patch sheet material (Fig. 1A), which has a yellowish hue and is a tough material in the dry state, with a reported elastic modulus of 83 kPa.[14] The SIS is a much softer material hydrated. SEM revealed the architecture of the SIS ECM material, namely its numerous collagen fibers and their random orientation (Fig. 1B–D). The multiple layers of the SIS could be seen on the edges of the patches (Fig. 1B), making it ideal for cell infiltration. Intact mASC cell monolayers were able to form on the patches (Fig. 1C). Cellular extensions to the collagen fibers could be seen, verifying cell adhesion to the ECM material (Fig. 1D).

To determine correlation of luminescent signal to cell numbers, increasing numbers of mASCs were plated into a six-well plate; D-Luciferin was added to the medium; and the plate imaged with an IVIS Spectrum system (Fig. 1E). A linear increase in luminescence signal correlated with a linear increase in cell numbers (Fig. 1F). This test also validated activity of the *Fluc* reporter gene in the cells. Using confocal microscopy, seeding depth of the ASCs into the SIS was found to be 89 ± 16 µm, which is over half of the 155-µm whole SIS thickness (Fig. 1G–I).

SIS significantly improves in vivo *stem cell survival*

BLI revealed a significant increase in cell survival and proliferation in wounds treated with a patch, evidenced by higher signal intensities (Fig. 2A, B). ASCs delivered with the patch removed 6 days after implantation proliferated the most in the wounds, with a peak in cell number at day 8 (purple line). Cell survival was notably reduced in cells delivered with the patch removed 2 days later (red line), followed by the remove and replace group (blue line). Initial signals (at day 2) in the patch groups differed, because in the remove day 2 and remove and replace groups, removing

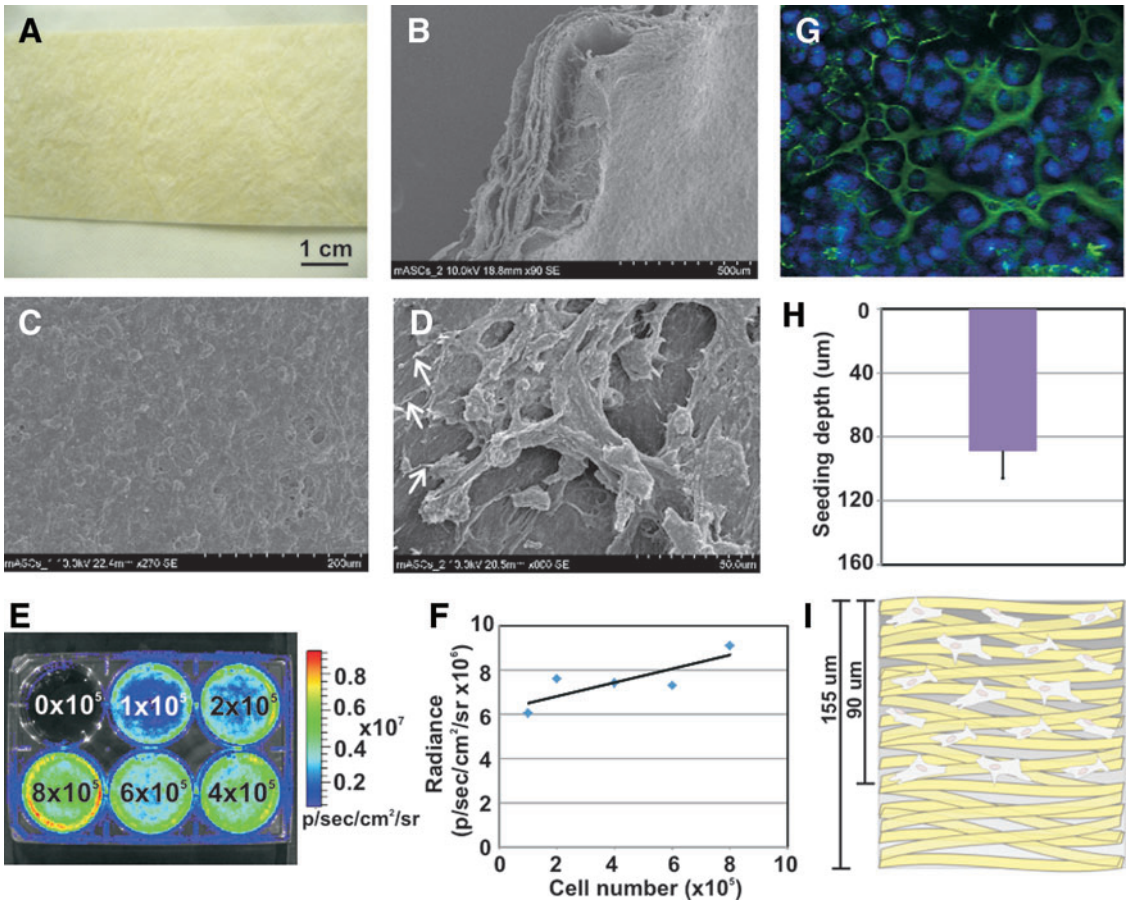

FIG. 1. Patch material and stromal cell characterization. **(A)** Gross image of the extracellular matrix (ECM) patch material. **(B–D)** Scanning electron microscopy images showing **(B)** the multiple layers of the patch and **(C, D)** adipose stromal cell seeding, with white arrows indicating cell attachments to the material. **(E, F)** Bioluminescence imaging (BLI) verification of cell signal; Luciferase + adipose-derived stromal cells (ASCs) plated at increasing numbers were bioluminescence imaged **(E)**, showing an approximately linear correlation between cell number and Luciferase signal **(F)**. These data verified cell signal and correlation of resultant luminescent signal. **(G–I)** Cell-seeding depth into the patch as determined by confocal imaging. **(G)** Cells stained with DAPI (blue) appeared to seed in and around the collagen fibers (autofluoresce green). **(H, I)** Cells were found to seed ~90-µm deep into the 155-µm-thick patch. Error bar = standard deviation. Color images available online at www.liebertpub.com/tea

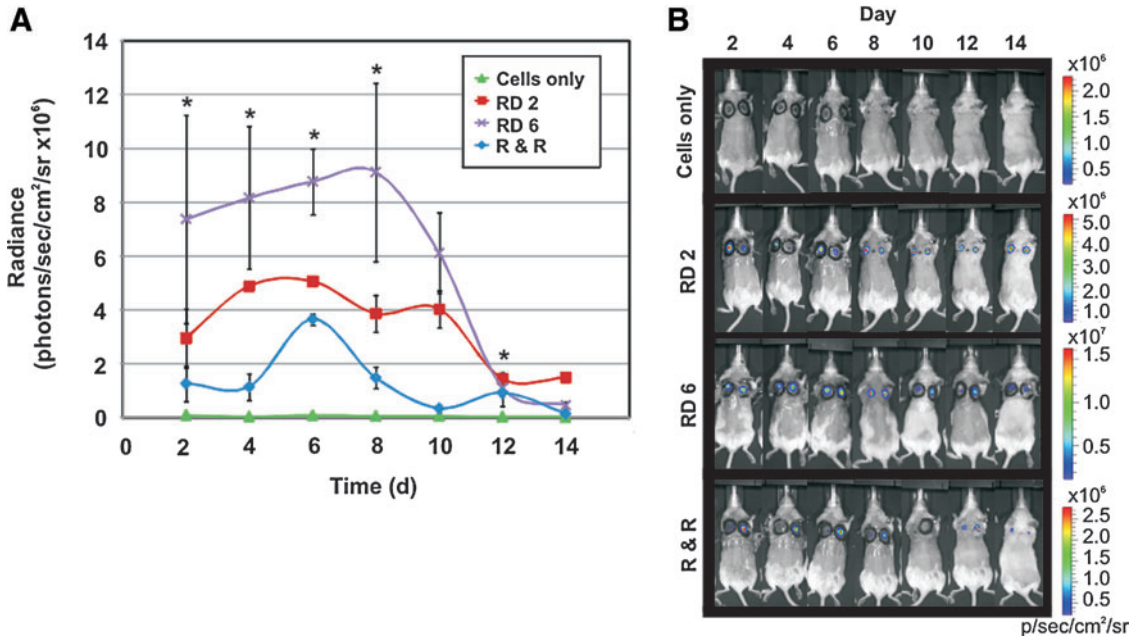

FIG. 2. BLI results for transplanted stem cells with and without the patch material. **(A)** Radiance signals from Luciferase activity in the transplanted ASCs, representing stem cell survival and proliferation. Cells in the remove day 6 group (RD 6, purple line) survived and proliferated significantly more than cells in all other groups for the majority of the time period. Cell survival and moderate proliferation were also seen in the remove day 2 (RD 2, red line) and remove and replace (R & R, blue line) groups, though less so than in the RD 6 group. ASCs in the cell-only group (green line) did not survive well. **(B)** Representative BLI images of resultant Luciferase signals from transplanted stem cells in the wounds. Error bars = standard deviation. *indicates statistical significance compared to untreated wound controls, $p < 0.05$. Color images available online at www.liebertpub.com/tea

patches before imaging removed cells along with the patch, as shown by the decrease in cell signal (Fig. 2A). In these groups, patches were removed before imaging to better model patient application where the patch would be removed on day 2. Cells transplanted alone did not survive in the wounds (green line), with little-to-no Luciferase signal. All cells on patches showed initial cell proliferation, followed by a decline, as the transplanted cells began to die, an observation often seen with transplanted stem cells. By day 12 postwounding, a loss in signal indicated that most ASCs had died by that time. Interestingly, cells in the remove day 2 group survived the longest in the wounds, though proliferation was much lower than in the remove day 6 group. Cells in the remove and replace group proliferated between days 4 and 6, and declined thereafter. Wound reinjury as the patch was removed every 2 days likely detached newly formed superficial layers of epithelium.

Stem cell application with the patch moderately improves healing

Wound closure rates are shown in Figure 3. Groups were compared to the control of untreated wounds (black lines). Stem cells alone topically applied to wounds did not improve healing rates (Fig. 3A). Delivering stem cells on the SIS patch slightly improved healing, though not significantly (Fig. 3B–D). The patch-only treatment hindered healing (Fig. 3E), as the patch stented the wound open as it attempted to heal. The remove day 6 group showed a gradual, modest increase in wound-healing rates, though only healing on day 4 was significantly improved (Fig. 3C). Wound closure measurements from day 0–6 in the remove day 6 group could be made despite the presence of the patch due to the semitransparency of the hydrated patch. Both remove day 2 and remove and replace groups showed no healing initially (Fig. 3B, D), as the skin was reinjured by removal of the patch during the early stages of wound healing. Significant differences in healing were seen in the remove and replace group near the end of the wound-healing process, from days 8–12 (Fig. 3D). This improvement is obscured by the lack of healing from days 0–4, negating the usefulness of this treatment regime. With the exception of the patch-only group, all groups exhibited complete healing, or full wound closure, by day 14. Patch application in all relevant groups typically continued until day 6, when the patch would dehydrate and detach from the wound. Differences in wound closure rates for each group compared to the wound-only control are shown in Figure 3F to illustrate the relative change in healing rates. The remove day 6, remove day 2, and remove and replace groups showed a positive increase in wound-healing rates, or improved healing. The remove day 6 group resulted in the largest overall increase in healing rates. Gross images of the wounds over the healing period are shown in Supplementary Fig. S1 (Supplementary Data are available online at www.liebertpub.com/tea).

Areas of fibrosis decreased

Fibrosis is the formation of scar tissue from the generation of *de novo* collagen and other ECM components during the proliferative phase of wound healing to form a provisional matrix. This leads to re-epithelialization where epithelial cells

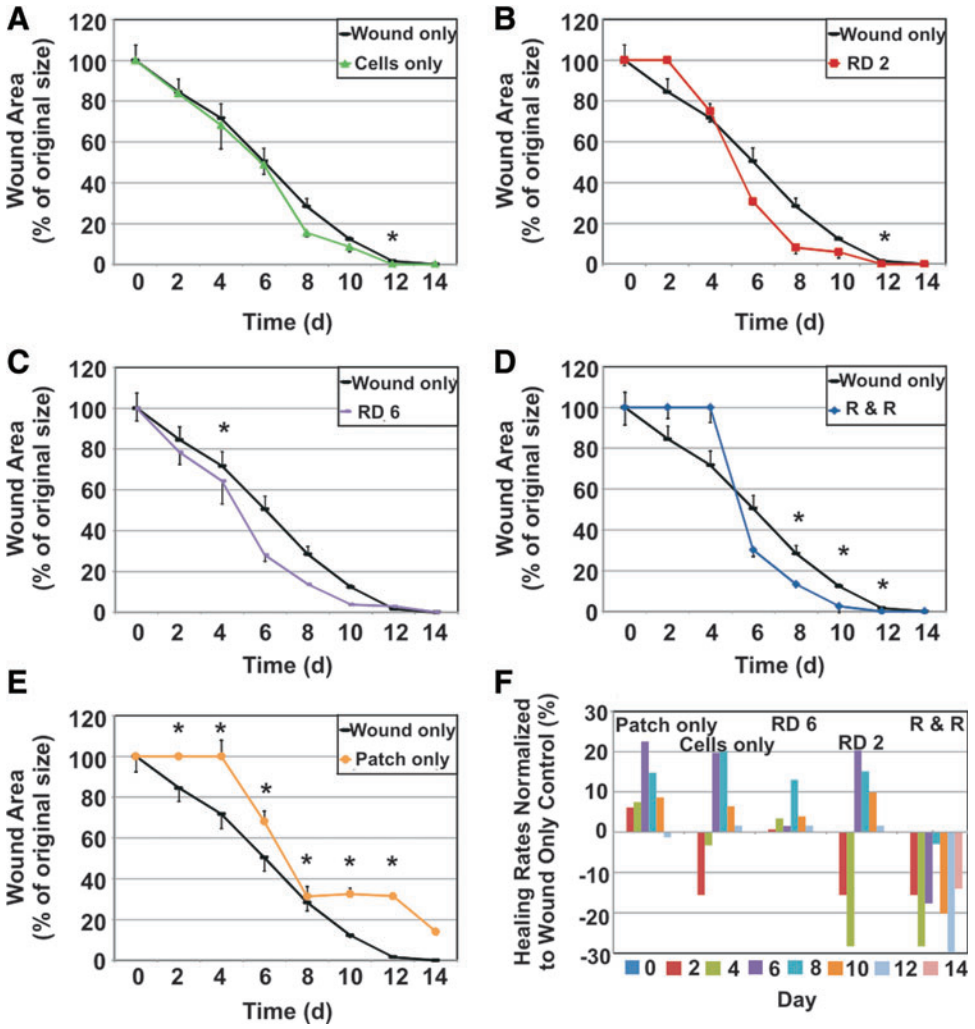

FIG. 3. Wound closure rates for all treatment groups versus untreated wound control. Wound closure rates are reported as a percent wound area of original size. Increased healing rates fall below the control wound only line (black line). In contrast, decreased healing rates appear above the black control line. **(A)** Stem cell-only treatment (green line) healing rates did not differ from control. **(B)** Removing the stem cell-seeded patch after 2 days (red line) showed no healing before day 2, as reinjury occurred once the patch was removed; slightly increased healing was seen post day 4. **(C)** In the RD 6 group (purple line), treated wounds showed a slight increase in healing rates, with significant results on day 4. **(D)** Initially, treating with a cell-seeded patch and replacing with a patch alone (no added cells) every 2 days (blue line) resulted in delayed healing, followed by a modest though significant increase in healing, showing a slight positive effect of continued patch treatment after stem cell application. **(E)** Patch-only treatment (orange line) resulted in decreased healing, as the patch stented the wound open, preventing wound closure. **(F)** To compare healing rates between groups, healing percentages were normalized to the wound only control. Bars above the x-axis represent increased healing rates, whereas bars below the x-axis represent decreased healing rates in comparison to the untreated control. Patch-only, RD 2, and R & R groups showed negative or decreased healing. Cell-only and RD 6 groups showed positive or increased healing, with larger positive differences in the RD 6 group. Error bars = standard deviation. *indicates statistical significance compared to untreated wound controls, $p < 0.05$. Color images available online at www.liebertpub.com/tea

migrate across the wound bed from the edges toward the center, replacing the provisional matrix with an organized and stratified epithelium.[15] All wounds in the six control and experimental groups exhibited differing amounts of fibrosis (Fig. 4A). Smaller areas of fibrosis indicate histological evidence of less scarring. Densely packed collagen, indicating fibrosis, was identified by 3 different staining techniques to ensure robustness in results: H&E (pink/purple collagen fibers), Masson's Trichrome (blue collagen), and Picrosirius Red (red collagen). Fibrosis region dimensions were measured, and the area was calculated. Fibrosis regions are demarcated by the black boxes (Fig. 4A). The smallest scar width was seen in the remove day 6 group (Fig. 4B). Fibrosis region depths were lowest in the remove day 2 group, followed by the remove and replace group (Fig. 4C). Compared to untreated wounds, fibrosis areas were significantly smallest in the remove day 2 group, closely followed by the cells only and remove day 6 groups (Fig. 4D). The remove and replace and wound-only groups exhibited comparable amounts of scar, with the patch-only group showing the largest amount of scar. Scar measurements were verified by an additional blinded researcher to strengthen confirmation

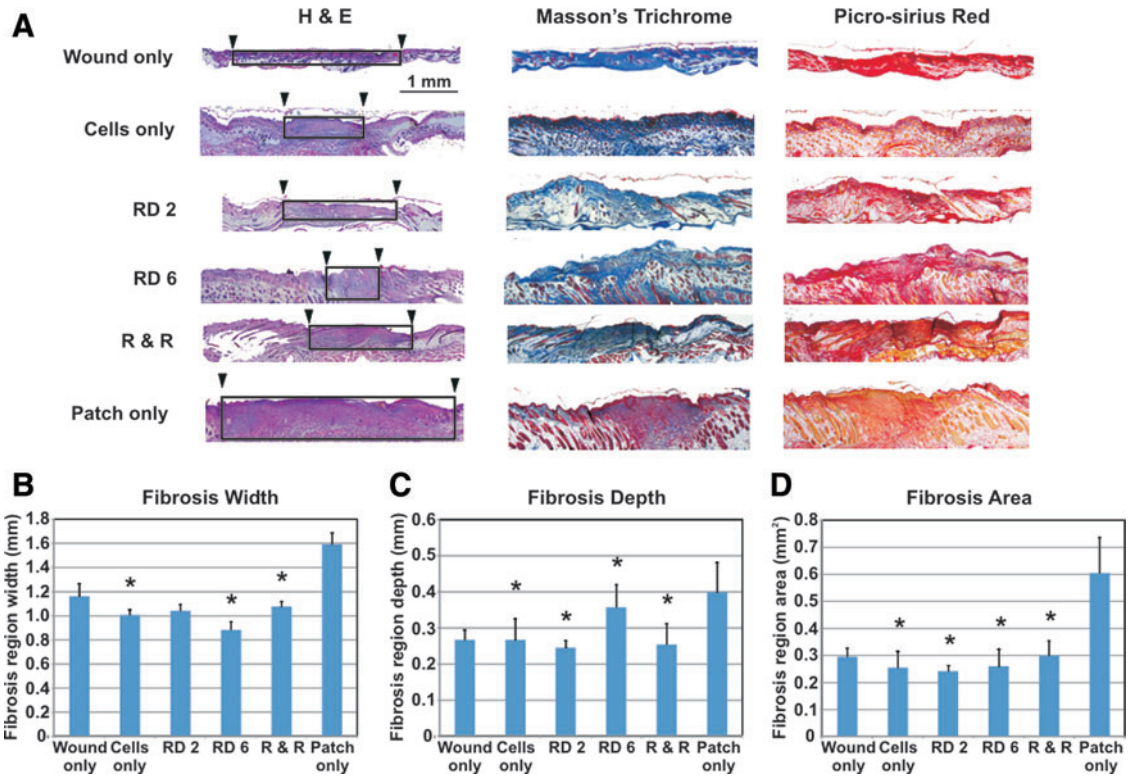

FIG. 4. Histological results for areas of fibrosis, or scarring, after full wound closure (day 14). **(A)** Histological staining revealed many collagen fibers, indicative of fibrosis (collagen fiber staining colors: H&E- pink/purple; Masson's Trichrome- blue; Picrosirius Red- red). In the H&E images, the width of fibrosis areas is marked by black arrowheads and black boxes approximate fibrotic areas. **(B)** Fibrosis region widths showed significant decreases in scarring in the cell-only, RD 6, and R & R groups compared to the wound-only control; the RD 6 group exhibited smallest fibrosis width. **(C)** Fibrosis region depths compared to wound-only control were significantly less in the cell-only, RD 2, RD 6, and R & R groups; smallest fibrosis depth regions were seen in the RD 2 group. **(D)** Fibrotic areas were significantly decreased in the cell-only, RD 2, RD 6, and R & R groups compared to the untreated wound-only group, signifying decreased scarring. Overall, smallest areas of fibrosis resulted from the RD 2 group, closely followed by the cell-only and RD 6 treatments. Patch-only treatment resulted in the largest scars. Error bars = standard deviation. *indicates statistical significance compared to untreated wound controls, $p < 0.05$. Color images available online at www.liebertpub.com/tea

in results. Both sets of measurements followed the same trend; the additional measurement data are shown in Supplementary Fig. S2.

Transplanted stem cells do not remain in wounds long term

To determine presence of any remaining transplanted stem cells posthealing, tissue sections from day 14 from all groups were stained with anti-GFP and DAPI, and then fluorescence imaged (Fig. 5). Results showed many DAPI-positive cells, though no colocalization with GFP signals, suggesting that no transplanted cells remained at day 14. BLI results at day 14 of low cell numbers confirm this finding (Fig. 2A). GFP signals present mostly derived from natural autofluorescence from collagen fibers. Small GFP-positive specks were seen, perhaps indicating remnant cell fragments from the transplanted ASCs. Larger fluorescent structures appeared to be the ECM material such as collagen and larger cells such as hair follicles that had formed during and after healing. These structures are especially evident in the remove day 6 group, with elongated, elliptical-shaped cells representative of hair follicles, indicating advanced healing. Except for the remove day 6 group, more collagen was seen in all groups, signifying more fibrosis. GFP signals in the wound-only group originated from autofluorescent ECM components.

According to the BLI results, transplanted stem cells survived well in the leading group (remove day 6) until day 8 (Fig. 2A), after which cell numbers steadily declined. To investigate presence of ASCs during early time points, wound samples were taken from the highest cell proliferation and survival group (remove day 6) at days 2, 4, 6, 8, and 10 postwounding and stained with anti-GFP and DAPI. Results were positive for GFP and DAPI colocalization, indicating presence of transplanted ASCs in the wound areas at all these time points, though the number of stain-positive cells remained low (Supplementary Fig. S3). Alternatively, low cell numbers may be due to GFP signal loss in the transplanted cells, making them difficult to discern via fluorescence imaging, and not due to the actual loss of stem cells. Transfected GFP signal loss by transplanted cells has been known to occur.[16] During early time points, areas around the wound were mainly composed of the ECM material and had few cells, as extensive cell infiltration into the wounded areas had not yet occurred (Supplementary Fig. S3).

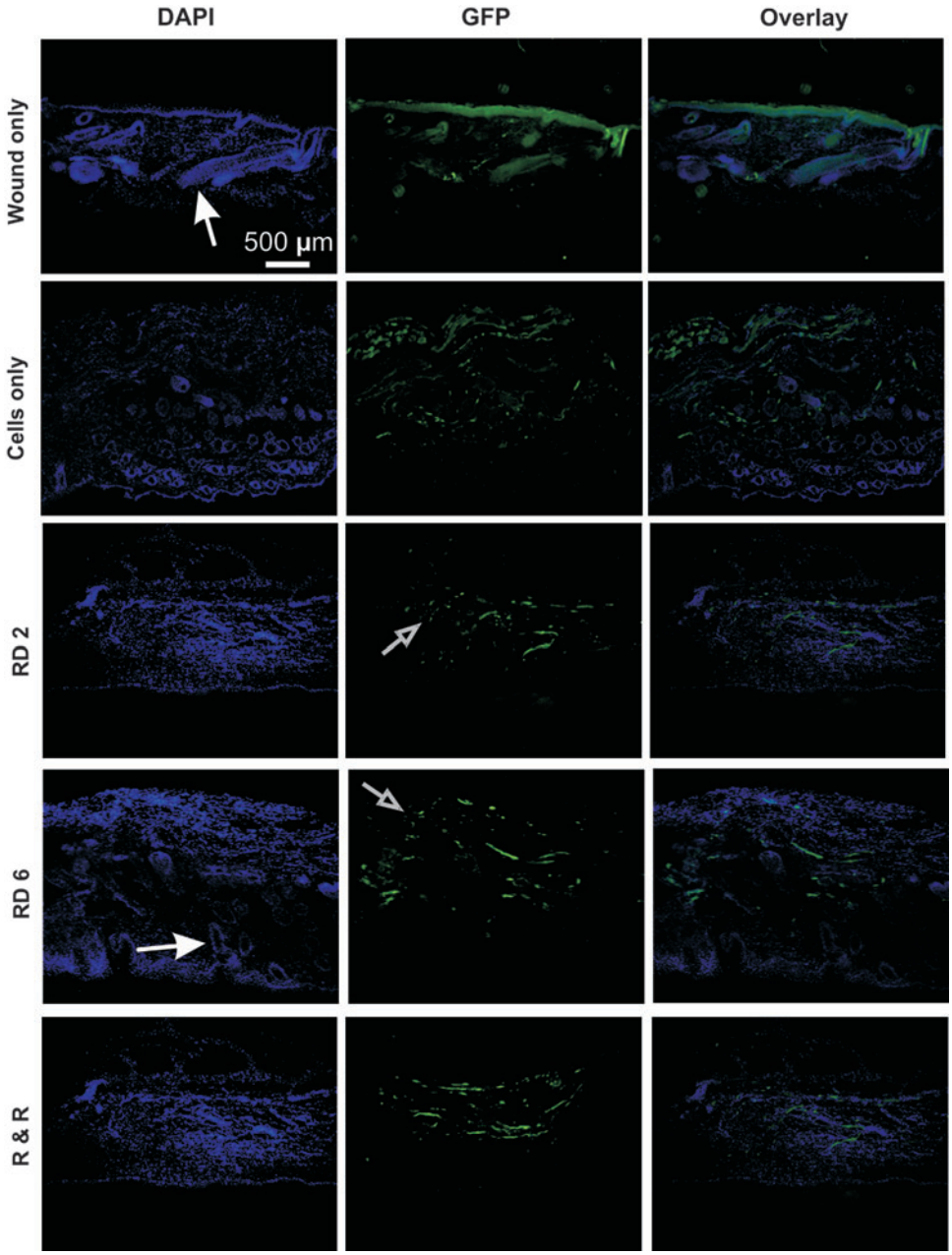

FIG. 5. Immunofluorescence results for DAPI and anti-green fluorescent protein (GFP) staining, marking transplanted stem cells at the end of the healing period, that is, day 14. Results were similar in all cell groups. DAPI-positive results mostly derived from resident cells (e.g., fibroblasts and keratinocytes) and large hair follicles (indicated by closed white arrows). GFP signals originated primarily from autofluorescent ECM components (e.g., collagen). Positive DAPI and GFP staining did not colocalize (as seen in the overlay images), suggesting that transplanted cells were no longer present at full wound closure. Small cell fragment-sized GFP signals are indicated by open arrows, suggesting that only transplanted stem cell fragments remained. Color images available online at www.liebertpub.com/tea

Discussion

Here, we showed that stem cell delivery along with an extracellular patch can improve cell survival and proliferation in skin wound healing. Additionally, fibrosis was significantly reduced. The excisional mouse wound healing model was chosen as it is constructed to closely mimic human wound healing.[13] This model also allows for relatively high-throughput screening as the mouse skin completely heals from full-thickness wounds in relatively rapid 2 weeks. In comparison to the wound-healing model used by Liu *et al.*,[8] their model lacked a wound split, hence the healing mechanisms were more murine-like in nature where contracture is the more prominent means of wound closure. In human wound healing, contracture is minimally present as wounds are allowed to heal via granulation, as in the case of the wound healing model we used in these studies.[17]

The random collagen fibril arrangement in the SIS is somewhat similar to the architecture of natural, developmental-stage collagen fiber orientation in scarless skin. In scar tissue, collagen is densely aligned unidirectionally, changing the appearance of the local wound area once healed. The SIS fiber arrangement may help to reduce scarring because of this random collagen arrangement, allowing cells to migrate and lay down epithelium similar to the original, unwounded tissue. More importantly, the SIS allowed the stem cells to remain localized to the wound area rather than migrate to other regions as evidenced by the BLI cell signals seen concentrated around the wound area. Initially, delivering the stem cells on the patch physically retained the cells to the wound area to maximize healing. Additional benefits of the patch are that it is natural, nonimmunogenic, hemostatic, pliable, and easily suturable—all factors that are important for translating this technology to human treatment.

Clinically, the SIS is implanted *in vivo* after hydration, typically with saline. The cell medium served as the SIS hydration liquid. After application to the skin wounds, the SIS material would begin to dry approximately on day 6. Additionally, stem cell survival as seen by the BLI results peaked at day 8 and steadily declined thereafter in all groups. Hence, time points later than day 6 for removing the patch were not investigated. Also, in terms of patient care, shorter application times are preferred because of the likelihood of the treatment and related dressings being disturbed.

Wounds treated with the patch only allowed for determination of the independent effect of the SIS and its components, including its growth factors. Leaving the patch on for the longest period possible tested the maximal potential effect of the patch. Patch-only treatment resulted in the slowest healing rates, due to the material stenting the wound open. Any positive effect of the material's growth factors or ECM components was over-ridden by the physical properties of the SIS. In the patch-only group, healing plateaued after day 8, suggesting that wound healing mechanics were stifled if the wound was left stented up to day 6, when the patch had dried and fallen off the wound. Healing continued past day 8 in the remove and replace group despite the presence of the patch, likely because of the benefit of the stem cells in the healing process. During early time points in the remove and replace group, the wound bed remained noticeably red after patch removal, representing neovascularization, or formation of blood vessels in response to reinjury. By leaving the cell-seeded patch on the wound until day 6, the stem cells remained localized to the wound, and ample time was allowed for healing.

Transplanted stem cell migration into the tissue is supported by the BLI data. After removal of the cell-seeded patch, a noticeable cell signal in the wound remained. This is especially evident in the remove day 6 group, where cells continued to proliferate until day 8, 2 days after patch removal. On day 8, when all groups with stem cells were near full wound closure, transplanted cells began dying as shown by the decrease in BLI signals. This may indicate that the stem cells had reached their potential in aiding the healing process, were no longer needed, and subsequently digested by inflammatory cells present in the granulation tissue.[1] ASC migration into the wounds was also seen at early time points. GFP-positive ASCs were seen located away from the SIS patch and deeper into the wound.

In the remove day 2 and remove and replace groups, patches were removed before imaging to approximate that patient treatment should the patch with cells be removed on day 2. BLI results showed that removing the patch on day 2 had a notable decrease in cell signal, indicating that many cells had been removed along with the patch. These data demonstrate that there was not sufficient time for cell migration from the patch into the wound by day 2; thus, patch removal at this time point would not be desirable.

ASCs were seeded at a density of 1×10^6 cells per 6-mm patch. The number of cells was chosen to saturate seeding. Lower cell number trials, such as 5×10^5 cells, resulted in less cells depositing onto the patch and uneven seeding (data not shown). Chances for stem cell rejection were minimized by implanting cells from mice with the same background as recipient mice. The loss of transplanted stem cells after full wound closure is not unusual. This phenomenon is commonly seen with transplanted stem cells, as they do not tend to survive for long periods of time *in vivo*. However, based on our results, the patch material elongated the time of survival of the stem cells in the wounds long enough to create a noticeable positive effect on healing.

As seen by Liu *et al.*, increased vascularization was found after stem cell transplantation on the SIS to a wound.[8] Hence, angiogenesis may have played a role in decreasing fibrosis in our study, by providing increased blood flow and perhaps in turn increasing native cell recruitment for regenerating and repairing the wounded tissue. Additionally, it is widely believed that stem cells most likely secrete paracrine factors such as growth factors, whereas in a wound site, promoting tissue repair. Of particular relevance, Lee *et al.* found that paracrine factors released by ASCs in culture increased proliferation of keratinocytes and dermal fibroblasts.[18] A similar mechanism may have likely occurred in our study to encourage tissue regeneration rather than fibrosis formation via local cell proliferation prompted by the paracrine effect.

Histological results revealed evidence of re-epithelialization and new collagen formation, indicating scar formation. The remove day 2 group exhibited the least amount of fibrosis, closely followed by the cell-only and remove day 6 groups. In consideration with cell survival and wound healing data, the remove day-6 treatment protocol may be most beneficial for improved patient care. In the remove and replace group, noticeable scar could be visibly seen. Reinjury by patch removal during the early stages of healing may have caused considerable additional tissue damage to the underlying dermis layer, increasing inflammation and scar formation. Naturally, excess scar formation is often seen in response to significant tissue damage.[19]

Although fibrosis was significantly reduced, healing rates were only slightly enhanced. Our delivery method showed an obvious increase in cell delivery and cell retention to the wounds. Changes to the materials and cells may further improve healing rates. Future improvements could involve investigating other material types, such as biodegradable polymers or other decellularized tissues, and other stem cell types.

Conclusions

We observed increased stem cell survival and significantly decreased areas of fibrosis by delivering stem cells with the ECM material. Wound closure rates were slightly improved. Clinically, the patch could be easily applied and conveniently covered with dressings. Based on our studies, this treatment would only need to last a few days (preferably removed after 6 days of application), during which the benefits of the stem cells could be administered, resulting in potentially less scar tissue and improved patient care. The patch is an attractive method for delivering stem cell treatments noninvasively, and could conceivably be used with a variety of stem cells and in other types of wounds.

Acknowledgments

We thank CorMatrix Cardiovascular, Inc., for kindly providing the SIS material. We would also like to thank the staff, in particular, Dr. Tim Doyle, of the SCi3 Small-Animal Imaging Service Center at Stanford for providing and maintaining the BLI facilities used for collecting some of the

data in this manuscript. We also thank Dr. Lydia Joubert of the Cell Sciences Imaging Facility for her assistance and training in SEM techniques. This work was funded by the Arthritis National Research Foundation, the Hagey Laboratory for Pediatric Regenerative Medicine, the Oak Foundation, the California Institute for Regenerative Medicine grant TB1-01190 (NPM), and the National Institutes of Health grants R33HL089027 (JCW) and T32 EB009035-02 (MTLam).

Disclosure Statement

No competing financial interests exist.

References

1. Shaw, T.J., Kishi, K., and Mori, R. Wound-associated skin fibrosis: mechanisms and treatments based on modulating the inflammatory response. Endocr Metab Immune Disord Drug Targets **10,** 320, 2010.
2. Quaglino, D., Jr., *et al.* Ultrastructural and morphometrical evaluations on normal human dermal connective tissue- the influence of age, sex and body region. Br J Dermatol **134,** 1013, 1996.
3. Ananta, M., Mudera, V., and Brown, R.A. A rapid fabricated living dermal equivalent for skin tissue engineering: an in-vivo evaluation in an acute wound model. Tissue Eng Part A **18,** 353, 2012.
4. Chen, F., *et al.* Cryopreservation of tissue-engineered epithelial sheets in trehalose. Biomaterials **32,** 8426, 2011.
5. Garric, X., *et al.* Potential of a PLA-PEO-PLA-based scaffold for skin tissue engineering: in vitro evaluation. J Biomater Sci Polym Ed 2011 [Epub ahead of print]. PMID: 21888762.
6. Cao, F., *et al. In vivo* imaging and evaluation of different biomatrices for improvement of stem cell survival. J Tissue Eng Regen Med **1,** 465, 2007.
7. Kutschka, I., *et al.* Collagen matrices enhance survival of transplanted cardiomyoblasts and contribute to functional improvement of ischemic rat hearts. Circulation **114,** I167, 2006.
8. Liu, S., *et al.* Synergistic angiogenesis promoting effects of extracellular matrix scaffolds and adipose-derived stem cells during wound repair. Tissue Eng Part A **17,** 725, 2011.
9. Li, Z., *et al.* Imaging survival and function of transplanted cardiac resident stem cells. J Am Coll Cardiol **53,** 1229, 2009.
10. Xu, Y., *et al.* Analysis of the material properties of early chondrogenic differentiated adipose-derived stromal cells (ASC) using an *in vitro* three-dimensional micromass culture system. Biochem Biophys Res Commun **359,** 311, 2007.
11. Freytes, D.O., *et al.* Biaxial strength of multilaminated extracellular matrix scaffolds. Biomaterials **25,** 2353, 2004.
12. Voytik-Harbin, S.L., *et al.* Identification of extractable growth factors from small intestinal submucosa. J Cell Biochem **67,** 478, 1997.
13. Galiano, R.D., *et al.* Quantitative and reproducible murine model of excisional wound healing. Wound Repair Regen **12,** 485, 2004.
14. Leng, Y., Ding, Z., and Gong, L. [Elastic modulus of small intestinal submucosa]. Zhongguo Xiu Fu Chong Jian Wai Ke Za Zhi **20,** 292, 2006.
15. Laplante, A.F., *et al.* Mechanisms of wound reepithelialization: hints from a tissue-engineered reconstructed skin to long-standing questions. FASEB J **15,** 2377, 2001.
16. Harvey, K.J., Lukovic, D., and Ucker, D.S. Membrane-targeted green fluorescent protein reliably and uniquely marks cells through apoptotic death. Cytometry **43,** 273, 2001.
17. Wong, V.W., Sorkin, M., Glotzbach, J.P., Longaker, M.T., and Gurtner, G.C. Surgical approaches to create murine models of human wound healing. J Biomed Biotechnol **2011,** 1, 2011.
18. Lee, S.H., Jin, S.Y., Song, J.S., Seo, K.K., and Cho, K.H. Paracrine effects of adipose-derived stem cells on keratinocytes and dermal fibroblasts. Ann Dermatol **24,** 136, 2012.
19. Barandon, L., *et al.* Secreted frizzled-related protein-1 improves postinfarction scar formation through a modulation of inflammatory response. Arterioscler Thromb Vasc Biol **31,** e80, 2011.

Address correspondence to:
Mai T. Lam, PhD
Department of Surgery
Stanford University School of Medicine
257 Campus Drive
Stanford, CA 94305

E-mail: mtlam@stanford.edu

Received: August 7, 2012
Accepted: October 3, 2012
Online Publication Date: November 16, 2012